AMS-02 data confront acceleration of cosmic ray secondaries in nearby sources

Mertsch, Philipp; Sarkar, Subir

Published in:
Physical Review D (Particles, Fields, Gravitation and Cosmology)

DOI:
10.1103/PhysRevD.90.061301

Publication date:
2014

PHYSICAL REVIEW D **90,** 061301(R) (2014)

AMS-02 data confront acceleration of cosmic ray secondaries in nearby sources

Philipp Mertsch[1] and Subir Sarkar[2,3]

[1]*Kavli Institute for Particle Astrophysics & Cosmology, 2575 Sand Hill Road, M/S 29, Menlo Park, California 94025, USA*

[2]*Rudolf Peierls Centre for Theoretical Physics, University of Oxford, 1 Keble Road, Oxford OX1 3NP, United Kingdom*

[3]*Niels Bohr Institute, Copenhagen University, Blegdamsvej 17, 2100 Copenhagen Ø, Denmark*

(Received 3 February 2014; published 9 September 2014)

We revisit the model proposed earlier to account for the observed increase in the positron fraction in cosmic rays with increasing energy, in the light of new data from the Alpha Magnetic Spectrometer (AMS-02) experiment. The model accounts for the production and acceleration of secondary electrons and positrons in nearby supernova remnants which results in an additional, harder component that becomes dominant at high energies. By fitting this to AMS-02 data we can calculate the expected concomitant rise of the boron-to-carbon ratio, as well as of the fraction of antiprotons. If these predictions are confirmed by the forthcoming AMS-02 data it would conclusively rule out all other proposed explanations, in particular, dark matter annihilations or decays.

DOI: 10.1103/PhysRevD.90.061301 PACS numbers: 98.70.Sa, 98.38.Mz

I. INTRODUCTION

Recently the AMS-02 Collaboration has presented precision data on cosmic ray (CR) protons, helium, electrons, positrons and the boron-to-carbon ratio from the first two years of the space mission [1,2]. Some intriguing results from earlier experiments have *not* been corroborated; e.g. there seems to be no "break" in the proton and helium spectra at $\sim$200 GeV/n as had been claimed earlier [3]. However, the finding by PAMELA [4] of a rise in the positron fraction with energy above $\sim$10 GeV has been spectacularly confirmed [5].

This is of particular interest as the hardening of the positron fraction had been widely interpreted as due to the annihilation [6] or decay [7] of weak-scale dark matter (DM). Such interpretations, while very exciting as potential findings of new physics beyond the Standard Model, have faced intrinsic challenges; e.g. the (velocity-averaged) DM annihilation cross section is required to be much larger than the typical value which yields the observed DM abundance for a thermal relic. Moreover, the expected antiprotons are *not* seen so the annihilations or decays must be only into leptons which is rather unnatural. Subsequently, more direct constraints have been presented on the associated energy release [8,9], severely constraining DM interpretations. Astrophysical explanations (see [10] for a review) have therefore gained more currency with nearby pulsar wind nebulae being frequently implicated.

An interesting alternative suggestion is that a hard spectrum of *secondary* positrons can be produced by the standard sources of Galactic cosmic rays (GCRs), i.e. supernova remnants (SNRs) [11,12] (see also [13] for a related suggestion). This does not require a new class of sources and has the added advantage that it is easily falsifiable due to related signatures in other secondary species; e.g. a rise is also predicted at higher energies in the antiproton-to-proton ratio ($\bar{\mathrm{p}}$/p) [14] and the boron-to-carbon ratio (B/C) [15,16].

Until recently, such tests were hampered both by the lack of precision in CR data and also the inconsistency between different data sets. In this paper we consider only the recently presented AMS-02 data which not only have unprecedented statistics but also the smallest ever systematic uncertainties. Besides fitting to the B/C and $e^{\pm}$ data we present our model prediction for the $\bar{\mathrm{p}}$/p. We improve on earlier studies by computing all observables consistently, e.g. using the same nuclear cross sections for the source and propagation part of the calculation. (See e.g. [17] for a discussion of antiproton production cross sections.)

The remainder of this paper is organized as follows: In Sec. II we compute the contribution from the production and acceleration of secondaries in the source, i.e. SNRs. For the transport of all CR species in the ISM we use the GALPROP code, and we explain our approach in Sec. III. In Sec. IV we present our results for the positron fraction, the lepton fluxes, proton and helium fluxes, as well as B/C. In addition, for the antiproton-to-proton ratio where data from AMS-02 are expected soon, we compare to currently available PAMELA data. We conclude in Sec. V.

II. PRODUCTION AND ACCELERATION OF SECONDARIES IN THE SOURCE

It is generally believed that collisionless shock waves in SNRs are the dominant agent for acceleration of GCRs [18]. After the shock cannot contain particles anymore they diffuse through the interstellar medium (ISM), producing secondary particles by spallation on the interstellar gas. The

production of secondary particles *inside* SNRs has largely been ignored (see, however, [19]) since the total grammage of ambient matter that primary CRs traverse therein is much smaller than the grammage they traverse in the ISM. However, it was realized [11,12] that charged secondaries like positrons, antiprotons or boron nuclei partake in shock acceleration in much the same way as their parent primaries. However, whereas primaries are injected from the background thermal plasma only at the shock, secondary particles are produced up to $\mathcal{O}(1)$ diffusion scale length away. This leads to a different spatial distribution for their injection and is reflected in a secondary spectrum *harder* than the primary one due to the energy-dependent diffusion coefficient. Therefore, although subdominant in total number, secondaries produced in the SNR can have observable consequences at high enough energies.

Here, we consider the acceleration of primary and secondary CRs in the test-particle approximation of diffusive shock acceleration. In its own rest frame, the shock is at $x = 0$ and the Rankine-Hugoniot conditions determine the compression factor r which fixes the ratio of gas densities and velocities $n_+/n_- = r = u_-/u_+$ on either side of the shock. The evolution of the gyro-phase and pitch-angle averaged phase space density $f_i \equiv f_i(x, p)$ of species i is governed by the transport equation

$$\frac{\partial f_i}{\partial t} = -u\frac{\partial f_i}{\partial x} + \frac{\partial}{\partial x} D_i \frac{\partial f_i}{\partial x} - \frac{p}{3}\frac{\mathrm{d}u}{\mathrm{d}x}\frac{\partial f_i}{\partial p} - \Gamma_i f_i + q_i, \quad (1)$$

where from left to right, the terms on the right-hand side describe convection, spatial diffusion, adiabatic losses/gains, inelastic losses and injection by spallation of heavier species, $q_i = \sum_{j>i} c\beta_j n_{\mathrm{gas}} \sigma_{j\to i} f_j$.

We solve for the steady-state solutions, $f_i^{\pm} \equiv f_i(x \gtrless 0)$, separately in the upstream ($x < 0$) and downstream ($x > 0$) regions where $\mathrm{d}u/\mathrm{d}x \equiv 0$, and impose the boundary conditions $f_i^+ < \infty$ and $\partial f_i^-/\partial x \to 0$ for $x \to \infty$ as well as $f_i^- \to Y_i \delta(p - p_0)$ for $x \to -\infty$, where Y_i is the injected abundance of species i and p_0 the injection momentum. Assuming that $\Gamma_i D_i/u_\pm^2 \ll 1$ and $x\Gamma_i/u_\pm < x_{\max}\Gamma_i/u_\pm \ll 1$ (which amounts to requiring efficient acceleration of nuclei [15]), we find for the downstream solution

$$f_i^+(x, p) = f_i^0(p) + r(q_i^0(p) - \Gamma_i^- f_i^0(p))\frac{x}{u_+}, \quad (2)$$

where $q_i^0(p) \equiv q_i^-(x = 0, p)$ is the upstream injection term at the shock, and

$$f_i^0(p) = \int_0^p \frac{\mathrm{d}p'}{p'}\left(\frac{p'}{p}\right)^{\gamma} \mathrm{e}^{-\gamma(1+r^2)(D_i(p)-D_i(p'))\Gamma_i^-(p)/u_-^2} \times \left[\gamma(1+r^2)\frac{D_i(p')}{u_-^2} q_i^0(p') + \gamma Y_i \delta(p' - p_0)\right] \quad (3)$$

is the phase space density at the shock. Without spallation and inelastic losses, i.e. for $q_i = 0, \Gamma_i = 0$, the well-known test-particle solution of diffusive shock acceleration, $f_i \propto p^{-\gamma}$, is recovered, with the spectral index $\gamma = 3r/(r-1)$, i.e. $\gamma = 4$ for a strong shock ($r = 4$). For nonzero spallation and assuming that the diffusion coefficient is proportional to momentum $D_i(p) \propto p$ (i.e. Bohm diffusion), $f_i^0(p)$ will be harder than the source spectrum $q_i^0(p)$ by one power in momentum. This results in an *increase* of the fraction of positrons with energy, and this will also be the case for other secondary species like boron or antiprotons.

We make the simplifying assumption that after a time τ_{SNR}, the effective lifetime of the SNR, all downstream particles are released in a time much shorter than the time needed for the particles to reach the observer at Earth. The integrated downstream spectrum is

$$\frac{\mathrm{d}N_i}{\mathrm{d}p} = 4\pi \int_0^{\tau_{\mathrm{SNR}} u_+} \mathrm{d}x\, x^2 4\pi p^2 f_i(x, p) = 4\pi p^2 V\left[f_i^0 + \frac{3}{4} r\tau_{\mathrm{SNR}}(q_i^0 - \Gamma_i^- f_i^0)\right], \quad (4)$$

where $V = \frac{4\pi}{3}(\tau_{\mathrm{SNR}} u_+)^3$ is the downstream volume. We note that the term $-\frac{3}{4} r\tau_{\mathrm{SNR}}\Gamma_i^- f_i^0(p)$ in Eq. (4), as well as the exponential in Eq. (3), will lead to a suppression of the secondary contribution at very high energies.

III. TRANSPORT OF GALACTIC COSMIC RAYS

For the transport of CRs in the ISM we employ the GALPROP code [20] which numerically solves a transport equation similar to Eq. (1) but with the total downstream spectrum from Eq. (4) as the source term and with transport parameters (diffusion coefficient, gas densities, energy losses) appropriate for the ISM. The spallation on interstellar gas of primary CRs, which are already softer than the source spectrum due to escape losses, leads to further injection of secondaries. These secondaries themselves suffer escape losses and are therefore further softened. At low energies, where the secondaries produced and accelerated in the SNRs are subdominant, secondary-to-primary ratios such as the positron fraction, B/C and $\bar{\mathrm{p}}$/p, are therefore expected to fall with energy, as is in fact observed. However, at higher energies the harder secondaries begin to dominate and the secondary-to-primary ratios should start to *rise* with energy.

Given that SNRs occur at random in the Galaxy, the flux from a distribution of burstlike and pointlike sources will, in general, differ from the flux assuming a smooth source density. This is particularly important for high energy electrons and positrons which have limited propagation lengths due to synchrotron and inverse Compton losses. We have therefore performed the propagation of light nuclei and leptons in the three-dimensional, stochastic SNR mode of GALPROP and recorded the fluxes for a statistical ensemble of 25 different realizations of a pulsarlike [21]

source distribution. For lepton fluxes, the envelope of the fluxes is shown by the shaded bands in the following figures, while for nuclei they are sufficiently narrow and are therefore suppressed—we show this for illustration for the proton flux alone.

IV. RESULTS

There are several free parameters in our model that determine the source spectra, namely r, $u_{\pm}$, $\tau_{\rm SNR}$, $n_{\rm gas}$ as well as the diffusion coefficient $D = \beta c r_{\rm L}(p)/3 \simeq 3 \times 10^{22} K_{\rm B}\ ({\rm pc/GeV}) Z^{-1} B_{\mu{\rm G}}^{-1}\,{\rm cm^2\,s^{-1}}$, where $r_{\rm L}(p)$ is the Larmor radius. Here, $K_{\rm B} \sim B^2/\delta B^2$ parametrizes deviations from the Bohm value, arising e.g. because at late stages of the SNR evolution field amplification is less efficient. (Moreover the adopted test-particle limit is then a good approximation.) However, of these parameters, only the combination $K_{\rm B}/(u_-^2 B)$ enters into the secondary terms, so we fix $B_{\mu{\rm G}} = 1$ and $u_- = 5 \times 10^7\ {\rm cm\,s^{-1}}$, values typical of old SNRs, and vary only $K_{\rm B}$. Similarly, we fix $n_{\rm gas} = 2{\rm cm}^{-3}$ and test different values of $\tau_{\rm SNR}$.

In choosing the parameters that describe the propagation, we cannot rely on studies which do *not* consider the contribution from secondaries as this can be important even at the lowest energies for the B/C or $\bar{\rm p}$/p ratio. We therefore fit the relevant parameters in the following order. First, varying the source parameters $\tau_{\rm SNR}$ and D as well as the propagation parameters κ (the ISM diffusion coefficient at a reference rigidity 4 GV), δ (its spectral index) and ${\rm d}v/{\rm d}z$ (the gradient of the galactic wind), we attempt to simultaneously reproduce B/C and the positron flux. The proton spectral index and normalization are then fixed by fitting to the AMS-02 proton flux. Nuclear abundances relative to protons are adopted from earlier studies [22]; however, fitting helium data requires a spectral index $\gamma_{\rm He}$ harder by ~0.1 compared to that of other nuclei, γ, which is a known issue [3]. We fix the electron spectral index both above and below a fixed break energy of 7 GeV as is required by radio observations [23], and the normalization by fitting to the AMS-02 electron flux. The positron fraction, B/C, and $\bar{\rm p}$/p are then *predictions* of the model. We adopt the force-field approximation of Solar modulation [24], allowing for different modulation potentials for the various species within the commonly adopted range 0.2–0.8 GV. The half-height of the diffusion volume, $z_{\rm max}$, is always fixed to 3 kpc.

We can thus fix most of the model parameters; however, due to the limited energy range of available data, there remains some freedom concerning the maximum energy $E_{\rm max}$ (or, equivalently, rigidity $R_{\rm max}$). In DSA models where the maximum energy is age limited, it would be determined by the diffusion coefficient and shock velocity, but in models where it is escape limited, it is a complicated function of the age of the source. Since we expect the biggest contribution from mature supernova remnants where the diffusion coefficient is relatively large (as magnetic field amplification is no longer efficient) and the shock speed is relatively low [cf. Eq. (3)], we allow $R_{\rm max}$ to range between 1 and tens of TV.

TABLE I. Parameter values of the models adopted in our analysis, both for the source ($R_{\rm max}$, $K_{\rm B}$, $\tau_{\rm SNR}$, γ, $\gamma_{\rm He}$, $\gamma_{e,1}$ and $\gamma_{e,2}$) and for the galactic propagation [δ, κ and $({\rm d}v/{\rm d}z)$].

$R_{\rm max}$	1 TV	3 TV	10 TV
$K_{\rm B}$	16	5	8
$\tau_{\rm SNR}(10^4\ {\rm yr})$	5	4	4
γ	4.15	4.05	4.10
$\gamma_{\rm He}$	4.05	3.95	4.00
$\gamma_{e,1}$	3.6	3.6	3.6
$\gamma_{e,2}$	4.55	4.50	4.50
δ	0.65	0.75	0.70
$\kappa\ (10^{28}\ {\rm cm^2\,s^{-1}})$	2.80	2.00	2.10
$({\rm d}v/{\rm d}z)\ ({\rm km\,s^{-1}\,kpc^{-1}})$	5	15	15

We adopt a benchmark model with $R_{\rm max} = 1$ TV. The other model parameters adopted are shown in Table I (which also lists two other models we considered). In Figs. 1–3 our results are compared with AMS-02 data [2].

A point of difference with earlier studies [11,12,14,15] is that our model parameters are chosen to reproduce the shallower rise of the AMS-02 positron fraction (compared to PAMELA or Fermi-LAT data) at high energies which also allows a fit to the tempered rise in the positron flux

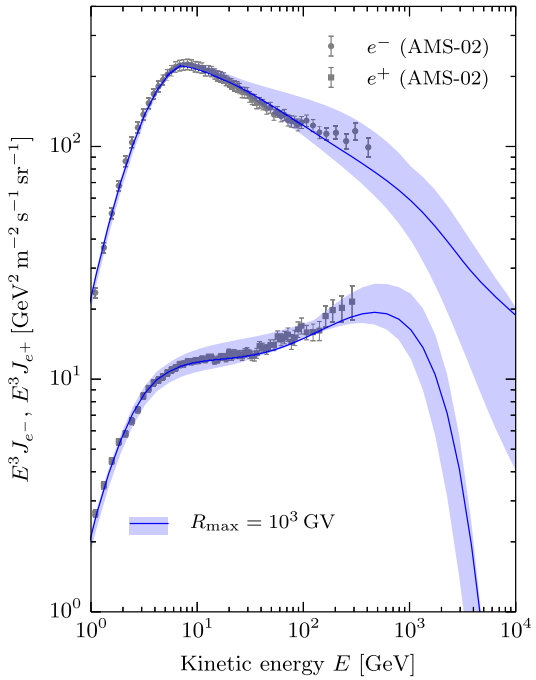

FIG. 1 (color online). Electron and positron fluxes measured by AMS-02 (circles and squares, respectively) and for the acceleration of secondaries model with maximum rigidity of 1 TV. The shaded band reflects the uncertainty of the spatial and temporal distribution of the SNRs.

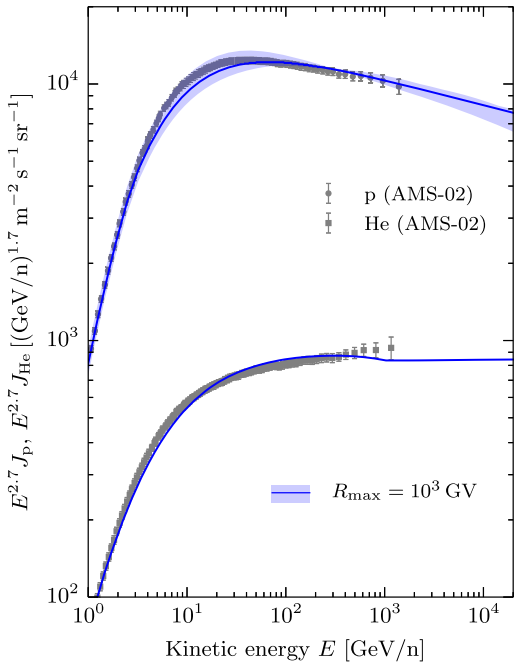

FIG. 2 (color online). Proton and helium fluxes measured by AMS-02 (circles and squares, respectively) and for the acceleration of secondaries model with maximum rigidity of 1 TV. The shaded band reflects the uncertainty of the spatial and temporal distribution of the SNRs.

shown in Fig. 1. We emphasise that reproducing this as well as the electron flux shown in the same figure is directly constrained by the fit to the proton and helium fluxes in Fig. 2. As seen in Fig. 3, both models provide good fits to the positron fraction measured by AMS-02.

To illustrate the spectral dependence on the maximum rigidity, we have varied the latter in the range 1…10 TV. Figures 4 and 5 show our results for $R_{\rm max} = 3$ and 10 TV together with those shown earlier for $R_{\rm max} = 1$ TV. In

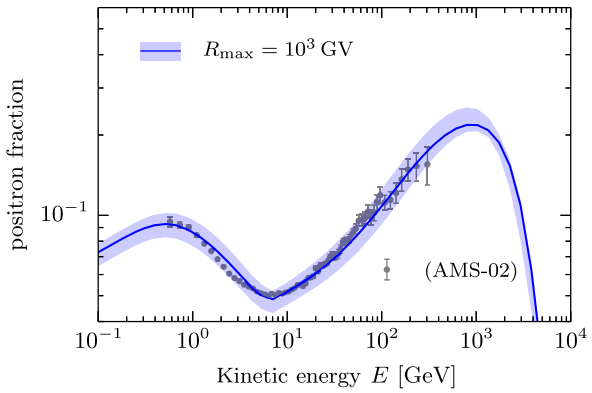

FIG. 3 (color online). The positron fraction $e^+/(e^+ + e^-)$ measured by AMS-02 (circles) and for the acceleration of secondaries model with maximum rigidity of 1 TV. The shaded band reflects the uncertainty of the spatial and temporal distribution of the SNRs.

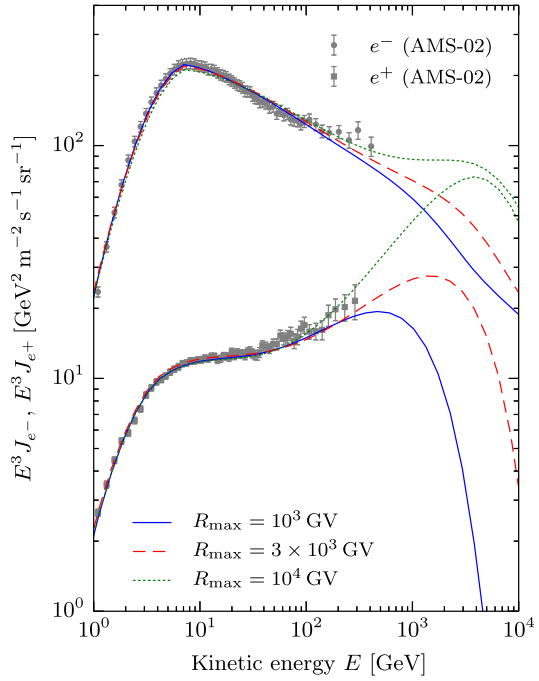

FIG. 4 (color online). Electron (circles) and positron (squares) fluxes measured by AMS-02 and predicted by the acceleration of secondaries models with maximum rigidities of 1, 3 and 10 TV.

Fig. 6, we compare the AMS-02 measurements with our prediction for B/C; we also show two recent balloon-borne measurements, viz. CREAM [25] and TRACER [26]. This displays the same behavior as the positron fraction—a fall at low energies where the (softer) boron flux produced by CR primaries in the ISM dominates, and a hardening at higher energies where the (harder) flux of borons produced and accelerated inside SNRs dominates. We also compare in Fig. 7 our antiproton-to-proton ratio to PAMELA data [27].

The other parameters for $R_{\rm max} = 3$ and 10 TV are shown in the third and fourth columns of Table I. Note that while $R_{\rm max}$ and $K_{\rm B}$ may be (anti)correlated, this depends in detail

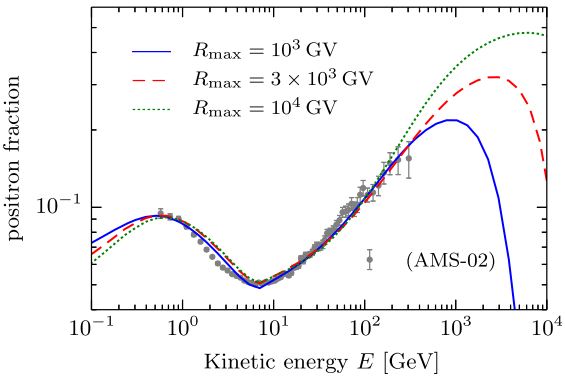

FIG. 5 (color online). The positron fraction $e^+/(e^+ + e^-)$ measured by AMS-02 (circles) and predicted by the acceleration of secondaries models with maximum rigidities of 1, 3 and 10 TV.

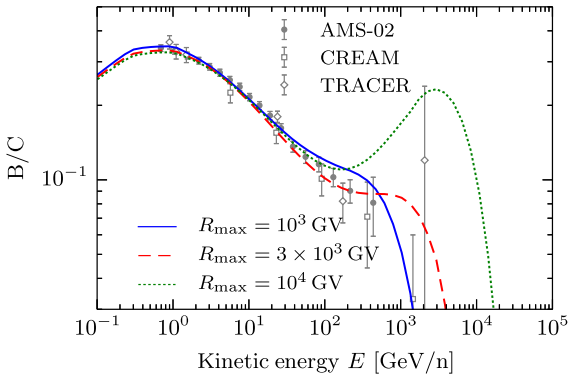

FIG. 6 (color online). The boron-to-carbon ratio measured by AMS-02 (circles), CREAM (open squares), TRACER (open diamonds), and predicted by the acceleration of secondaries models with maximum rigidities of 1, 3 and 10 TV.

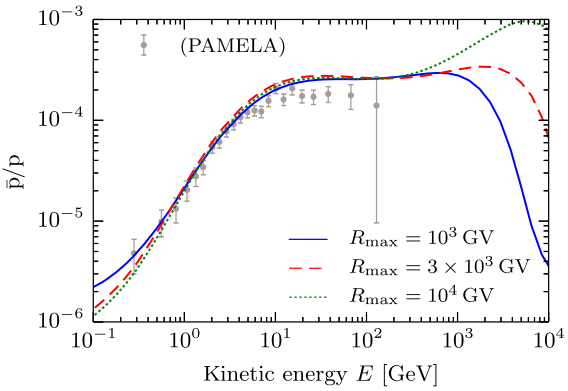

FIG. 7 (color online). The antiproton-to-proton ratio measured by PAMELA (circles) and predicted by the acceleration of secondaries models with maximum rigidities of 1, 3 and 10 TV.

on how the cosmic rays escape from the SNRs—in the absence of a firm understanding we have treated these as independent parameters (and let the fit to the data determine the value of $K_{\rm B}$). Also we have *not* done a comprehensive scan of all the parameters; hence, the curves do not always vary monotonically.

Given their limited energy range and uncertainties, the presently available electron and positron data (see Fig. 4) cannot pin down $R_{\rm max}$. However, Fig. 5 illustrates that higher energy measurements of the positron fraction with better statistics can distinguish between maximum rigidities of 1 TV and tens of TV. This is an important point as $R_{\rm max}$—if it is the same for all secondary species as is assumed here—leads to qualitatively different behaviors for B/C: While for $R_{\rm max} = 1$ TV, B/C shows only a slight hardening just below the cutoff, it flattens out for $R_{\rm max} = 3$ TV and even shows a characteristic rise for $R_{\rm max} = 10$ TV. The minimum in the latter case is close to the highest energy bin for which AMS-02 has presented data. Note that this minimum is at a *different* energy for B/C and for the positron fraction. This is due to the different kinematics (positrons are on average produced at $\sim 1/20$ of the parent primary energy, whereas in spallation the energy per nucleon is roughly conserved) and also to the spectral softening in the primary electron spectrum.

However, as seen in Fig. 7, the $\bar{\rm p}/{\rm p}$ fraction shows a flattening between tens and hundreds of GeV, unlike the positron fraction or B/C. At these energies, the antiproton flux is dominated by the secondary contribution which has the same spectrum as the primary species [cf. the term $4\pi p^2 V(3/4r\tau_{\rm SNR} q_i^0)$ in Eq. (4)]; the effect of the upper rigidity cutoff becomes apparent only at higher energies where the term $4\pi p^2 V f_i^0$ starts to dominate.

V. CONCLUSION

We have presented results for the (absolute) electron and positron, proton and helium fluxes, as well as B/C and $\bar{\rm p}/{\rm p}$, in the framework of the acceleration of secondaries by SNR shock waves models. The only free parameter that cannot be fixed by fitting to available data from AMS-02 is the maximum rigidity to which cosmic rays are accelerated by the SNR shock wave. Depending on whether it is high (e.g. 10 TV) or low (e.g. 1 TV), the positron fraction will keep increasing beyond a TeV, or cut off shortly above the highest energy bin for which results have been shown by AMS-02. This behavior should be reflected by a cutoff or a rise after a shallow minimum in B/C. For $\bar{\rm p}/{\rm p}$, we have found a plateau between tens and hundreds of GeV.

Our results differ significantly from Ref. [28] since these authors fixed $\delta = 0.43$ for the energy dependence of the ISM diffusion coefficient, whereas we have considered larger values in the range $\delta = 0.65$–0.75 as is expected in diffusion-convection models of CR transport [29]. This is essentially why we are able to consistently fit *both* the positron fraction and the B/C ratio. We await the release of AMS-02 data on the $\bar{\rm p}/{\rm p}$ and B/C ratios, which will definitively test all models proposed to account for the rising positron fraction.

ACKNOWLEDGMENTS

We are grateful to Stefan Schael for helpful discussions. P. M. is supported by DOE Contract No. DE-AC02-76SF00515 and a KIPAC Kavli grant made possible by the Kavli Foundation. S. S. acknowledges a grant from the Danish National Research Foundation.

[1] M. Aguilar *et al.* (AMS Collaboration), CERN Courier **53**, No. 8, 22 (2013); the web link of this article is http://cerncourier.com/cws/article/cern/54675 and it can also be found in the PDF issue: https://cds.cern.ch/record/1603700?ln=en.
[2] S. Haino, V. Choutko, A. Oliva, and S. Schael (AMS Collaboration), *Proceedings of the 33rd International Cosmic Ray Conference, Rio de Janeiro, 2013*, http://143.107.180.38/indico/contributionListDisplay.py?confId=0&filter=yes&selTypes=0&selSessions=3&selTracks=57&filterText=with%20AMS.
[3] O. Adriani *et al.* (PAMELA Collaboration), Science **332**, 69 (2011).
[4] O. Adriani *et al.* (PAMELA Collaboration), Nature **458**, 607 (2009).
[5] M. Aguilar *et al.* (AMS Collaboration), Phys. Rev. Lett. **110**, 141102 (2013).
[6] L. Bergstrom, T. Bringmann, and J. Edsjo, Phys. Rev. D **78**, 103520 (2008).
[7] E. Nardi, F. Sannino, and A. Strumia, J. Cosmol. Astropart. Phys. 01 (2009) 043.
[8] M. Ackermann *et al.* (LAT Collaboration), Astrophys. J. **761**, 91 (2012).
[9] M. S. Madhavacheril, N. Sehgal, and T. R. Slatyer, Phys. Rev. D **89**, 103508 (2014).
[10] P. D. Serpico, Astropart. Phys. **39**, 2 (2012).
[11] P. Blasi, Phys. Rev. Lett. **103**, 051104 (2009).
[12] M. Ahlers, P. Mertsch, and S. Sarkar, Phys. Rev. D **80**, 123017 (2009).
[13] Y. Fujita, K. Kohri, R. Yamazaki, and K. Ioka, Phys. Rev. D **80**, 063003 (2009).
[14] P. Blasi and P. D. Serpico, Phys. Rev. Lett. **103**, 081103 (2009).
[15] P. Mertsch and S. Sarkar, Phys. Rev. Lett. **103**, 081104 (2009).
[16] N. Tomassetti and F. Donato, Astron. Astrophys. **544**, A16 (2012).
[17] F. Donato, D. Maurin, P. Salati, A. Barrau, G. Boudoul, and R. Taillet, Astrophys. J. **563**, 172 (2001).
[18] P. Blasi, Astron. Astrophys. Rev. **21**, 70 (2013).
[19] E. G. Berezhko, L. T. Ksenofontov, V. S. Ptuskin, V. N. Zirakashvili, and H. J. Voelk, Astron. Astrophys. **410**, 189 (2003).
[20] I. V. Moskalenko and A. W. Strong, Astrophys. J. **493**, 694 (1998).
[21] D. R. Lorimer, arXiv:astro-ph/0308501.
[22] V. S. Ptuskin, I. V. Moskalenko, F. C. Jones, A. W. Strong, and V. N. Zirakashvili, Astrophys. J. **642**, 902 (2006).
[23] A. W. Strong, E. Orlando, and T. R. Jaffe, Astron. Astrophys. **534**, A54 (2011).
[24] L. Gleeson and W. Axford, Astrophys. J. **154**, 1011 (1968).
[25] H. S. Ahn, P. S. Allison, M. G. Bagliesi, J. J. Beatty, G. Bigongiari, P. J. Boyle, T. J. Brandt, J. T. Childers *et al.*, Astropart. Phys. **30**, 133 (2008).
[26] A. Obermeier, M. Ave, P. Boyle, C. Hoppner, J. Horandel, and D. Muller, Astrophys. J. **742**, 14 (2011).
[27] O. Adriani *et al.* (PAMELA Collaboration), Phys. Rev. Lett. **105**, 121101 (2010).
[28] I. Cholis and D. Hooper, Phys. Rev. D **89**, 043013 (2014).
[29] D. Maurin, A. Putze, and L. Derome, Astron. Astrophys. **516**, A67 (2010).